

Characteristics of point defects in the green luminescence from Zn- and O-rich ZnO

C. Ton-That,^{*} L. Weston, and M. R. Phillips*School of Physics and Advanced Materials, University of Technology, Sydney, P.O. Box 123, Broadway, NSW 2007, Australia*

(Received 15 March 2012; revised manuscript received 12 August 2012; published 10 September 2012)

Cathodoluminescence spectra have been measured to determine the characteristics of ubiquitous green luminescence (GL) in nonstoichiometric zinc oxide (ZnO). Zn- and O-rich ZnO were found to exhibit characteristic emissions at 2.53 eV [full width at half-maximum (FWHM) 340 meV] and 2.30 eV (FWHM 450 meV), respectively. Hydrogen was used to probe the physical nature of GL centers. The Zn-rich GL is enhanced upon H incorporation, whereas the O-rich GL is completely quenched as its underlying acceptor-like V_{Zn} centers are passivated by H. The GL emission bands each exhibit remarkably different excitation-power dependencies. The Zn-rich GL follows a close to linear relationship with excitation power, while the O-rich GL exhibits a square-root dependence. Calculations based on bimolecular recombination equations show the defect concentration in Zn-rich ZnO is three orders of magnitude greater than that in O-rich ZnO, indicating V_{O} is more readily formed than V_{Zn} in thermochemical treatments of ZnO.

DOI: [10.1103/PhysRevB.86.115205](https://doi.org/10.1103/PhysRevB.86.115205)

PACS number(s): 78.60.Hk, 71.55.Gs, 78.67.Bf

I. INTRODUCTION

Zinc oxide (ZnO), a semiconductor with a direct band gap of 3.37 eV and unique optical properties, is a leading material for next-generation light-emitting devices in the ultraviolet and blue spectral range. The material possesses superior properties, including large exciton binding energy (60 meV) and a low lasing density threshold,¹ combined with the availability of high-quality ZnO crystals for homoepitaxial growth.² ZnO can exhibit intense visible luminescence arising from impurities and defects,³ leading to its extensive uses in phosphor technologies. It is generally agreed that Li (a common impurity in hydrothermal growth) is responsible for yellow luminescence; however, the chemical origin of ubiquitous green luminescence (GL) remains controversial and has been attributed to several native defects, including oxygen vacancies (V_{O}),⁴ zinc vacancies (V_{Zn}),⁵ interstitials (Zn_i , O_i),⁶ and antisites (Zn_{O} , O_{Zn}).⁷ Density functional theory (DFT) calculations,^{5,8} however, indicated that the interstitial and antisite defects are unlikely the cause of GL since they have either too high formation energies (Zn_{O} , O_{Zn} , and O_i) to occur in any significant concentrations or form shallow levels (Zn_i). More recent papers suggested that there can be multiple emissions in the green spectral range,^{9,10} which accounts for often contradictory interpretations of the GL origin in the open literature.

Formation energies and concentrations of vacancy defects, and thus the luminescence properties, are theoretically predicted to be highly sensitive to the degree of nonstoichiometry in ZnO.⁸ This is supported by experimental data, which show deviations from stoichiometric ZnO can have pronounced effects on the GL emission energy and intensity.^{10,11} Although the impact of stoichiometry on GL is recognized, the physical nature of donors and/or acceptors dominating this emission remains puzzling. To elucidate defect-related GL in nonstoichiometric ZnO, we have investigated two types of ZnO: Zn- and O-rich particles that emit only GL. Most previous investigations were hindered from multiple defect-related emissions since the formation of point defects is sensitive to growth method and conditions.^{8,12} Annealing ZnO in oxidizing or reducing atmospheres, or controlled introduction of reactive dopants such as H, may be able to discriminate the defects responsible

for the GL. Such methods are the essence of this study. Plasma doping may be superior to ion implantation since the latter technique produces simultaneously structural disorder, which must be taken into account when considering the evolution of defect-related luminescence with changes in implantation dose and energy. Previous x-ray absorption near-edge structure (XANES) and cathodoluminescence (CL) studies have revealed a connection between the GL centered at 2.52 eV and V_{Zn} .¹³ In this paper, we offer experimental evidence that GL emission originates from different defects in O- and Zn-rich ZnO and provide insight into the characteristics of responsible defect centers based on a theoretical model of competitive recombination processes. The results provide a universal explanation for the GL in ZnO and help resolve a long-standing controversy on the role of point defects in this emission.

II. EXPERIMENTAL

Nonstoichiometric ZnO was used in this study. Zn-rich ZnO (from Phosphor Technology Ltd.) was produced by annealing particles in the presence of metallic Zn, while O-rich ZnO was obtained by annealing in pure O_2 gas at 1300 K. The particle sizes range from 0.5 to 1 μm . X-ray diffraction analysis of the particles reveals a single hexagonal wurtzite structure. To probe the charge state of GL defects, the particles were incorporated with H using mild hydrogen radio-frequency plasma (15 W, sample temperature 470 K). The samples were characterized by scanning CL microanalysis at 80 K using a FEI Quanta 200 scanning electron microscope (SEM) equipped with an Ocean Optics SD2000 diode array spectrometer. For excitation power density measurements, the accelerating voltage was fixed at 15 kV, while the injection current was varied in the range 30 pA to 10 nA. All spectra were corrected for the response of the system.

III. RESULTS AND DISCUSSION

A. Effects of stoichiometry on the luminescence properties

Figure 1(a) shows a representative SEM image of ZnO particles used in this CL study. The particles have different

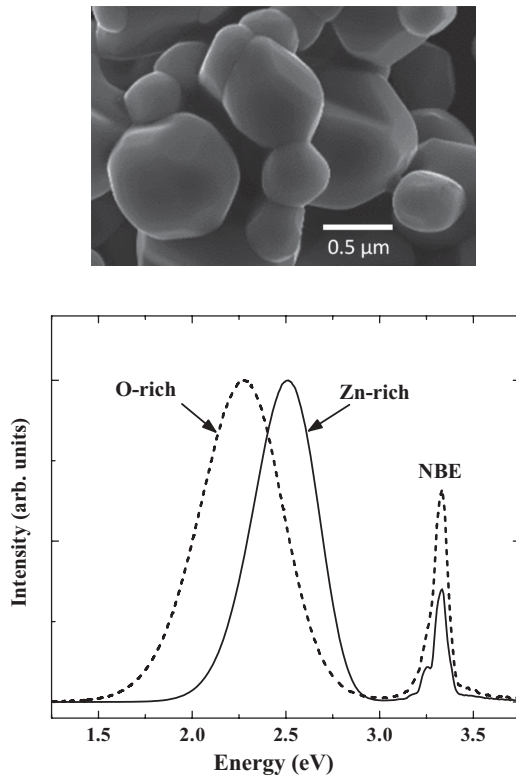


FIG. 1. (a) Representative SEM image of particles used in this study. (b) CL spectra of Zn- and O-rich ZnO particles at 80 K ($E_B = 15$ keV, $I_B = 0.25$ nA) normalized to the GL peak height. Both Zn- and O-rich ZnO exhibit NBE emission at 3.35 eV but different GL peak energies of 2.52 and 2.30 eV, respectively.

sizes with diameters in the range 0.5 to 1 μm , sufficiently large not to introduce quantum size effects, other than stoichiometric variations. The CL spectra of Zn- and O-rich ZnO, collected using a primary beam $E_B = 15$ keV and current $I_B = 0.25$ nA, are presented in Fig. 1(b). For ZnO, this beam energy corresponds to a CL sampling depth of 480 nm, as estimated by modeling the electron-energy-loss profile using the Monte Carlo stimulation CASINO.¹⁴ The simulation also accounts for the diffusion of minority carriers (diffusion length ≈ 98 nm [Ref. 15]). The dimensions of the CL generation profile are smaller than the lower limit of the particle size range; the GL emission thus arises mostly from the particle cores. This result is further verified using depth-resolved CL [Ref. 3] but contradicts the suggestion that the GL in ZnO nanostructures originates from their surfaces.¹⁶ Both samples show a near-band-edge (NBE) emission peaking at 3.35 eV, attributed mainly to recombination of free and donor-bound excitons.¹⁷ Phonon replicas are present on the low-energy side of the NBE separated by 72 meV, consistent with the longitudinal optical (LO) phonon mode in ZnO.¹⁷ The luminescence of both specimens is dominated by GL emission centered at 2.52 eV [full width at half-maximum (FWHM) 340 meV] and 2.30 eV (FWHM 450 meV) for Zn- and O-rich ZnO, respectively. These broad GL bands remain structureless as the temperature is decreased to 10 K, indicating that this emission is not associated with Cu impurity¹⁸ but originates from intrinsic point defects. The peak position and FWHM of Zn-rich GL are comparable with photoluminescence (PL)

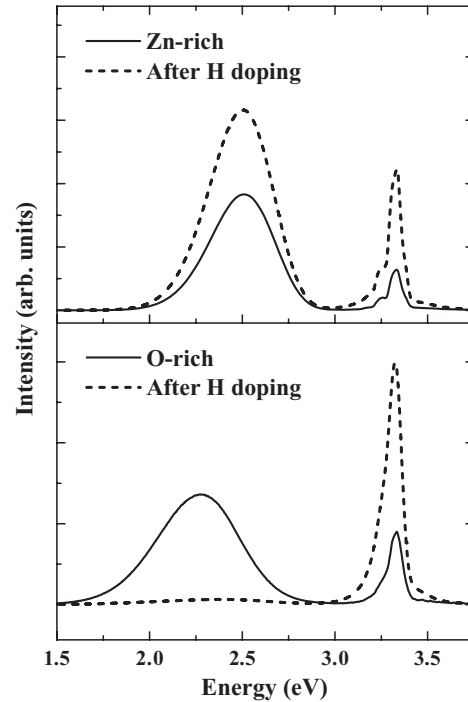


FIG. 2. Effects of H doping on the luminescence of Zn- and O-rich ZnO particles. While the NBE in both particles is enhanced due to passivation of nonradiative centers, the defect-related GL responds in an opposite fashion. The Zn-rich GL increases following H doping, whereas the O-rich GL is completely diminished.

studies by Leiter *et al.*,¹⁹ who attributed this emission to an anionic V_O from optically detected magnetic resonance. The wider FWHM of the O-rich GL is most likely due to the presence of multiple luminescence centers, namely V_{Zn} and V_{Zn} -related complexes, which have slightly different energies within the gap.⁹ Considering both the CL and PL findings and the fact that the particles are Zn-rich, the 2.52 eV GL emission can be assigned to V_O .

In order to probe the physical nature of the defects responsible for GL in Zn- and O-rich ZnO, both specimens were doped with H from a mild hydrogen plasma treatment at 470 K; a temperature where H is mobile in ZnO.²⁰ The H plasma did not affect the morphology or crystallinity of the particles but induced major changes to their luminescence properties. Figure 2 shows the CL spectra ($E_B = 15$ keV, $I_B = 0.25$ nA) of the particles at 80 K before and after exposure to 10 min of plasma. The NBE emission at 3.35 eV is significantly enhanced following hydrogen doping. Hydrogen is known to exist exclusively as a positively charged donor in ZnO.^{21,22} This enhancement has been attributed to passivation of competitive recombination pathways as well as the creation of additional radiative channels in the NBE region due to H shallow donors.^{23–25} The two GL emission peaks at 2.52 eV and 2.30 eV react to H^+ in an opposite fashion. The intensity of the Zn-rich GL at 2.52 eV increases due to the passivation of nonradiative defects. H plasma could also increase the concentration of V_O by extracting surface oxygen.²⁶ Conversely, the O-rich GL is totally quenched following H doping, suggesting a strong interaction of H^+ with defects responsible for the 2.30-eV GL emission. The

complete GL quenching by H also eliminates any role of Li impurity in this visible band as Li-related yellow luminescence is unaffected by hydrogen doping.²⁵ V_O and its complexes are all believed to be deep donors in ZnO, while V_{Zn} is considered to be an acceptor.²⁷ Although the nature of interaction between defects and hydrogen has not been conclusively established, as a positively charged H^+ in ZnO, it would interact favorably with acceptors rather than donors. Density functional theory calculations have suggested that hydrogen passivates V_{Zn} by formation of a thermodynamically stable $(V_{Zn}-H_2)^0$ complex, making the defect electrically inactive.²⁸ This prediction is consistent with the complete quenching of the O-rich GL after H doping. Based on these experimental results and theoretical predictions, the O-rich GL can be ascribed to V_{Zn} .

B. Dependence of GL intensities on CL excitation power

The O- and Zn-rich GL emissions were observed to exhibit remarkably different excitation-power dependencies as the beam current, I_B (i.e., excitation density), was increased from 0.03 nA to 10 nA, while the beam energy remains constant ($E_B = 15$ keV). Varying I_B in this range did not introduce any noticeable changes in peak shape or position, except for relative intensities of the NBE and GL, indicating that the exciton-exciton scattering loss is insignificant under the excitation conditions used.²⁹ The excitation-dependent behaviors of the O- and Zn-rich GL are illustrated in a log-log plot (Fig. 3) using a simple power-law model $I_{CL} \propto I_B^k$, where I_{CL} is the CL intensity. With increasing I_B , the intensity of the Zn-rich GL at 2.52 eV increases at a significantly faster rate than the O-rich GL intensity at 2.30 eV. Power-law fits reveal that the intensity of the O-rich GL shows a strongly sublinear dependence on I_B , with $k(\text{O-rich GL}) = 0.60 \pm 0.03$, while the Zn-rich GL exhibits an almost linear relationship with $k(\text{Zn-rich GL}) = 0.87 \pm 0.05$. The NBE emission in both specimens

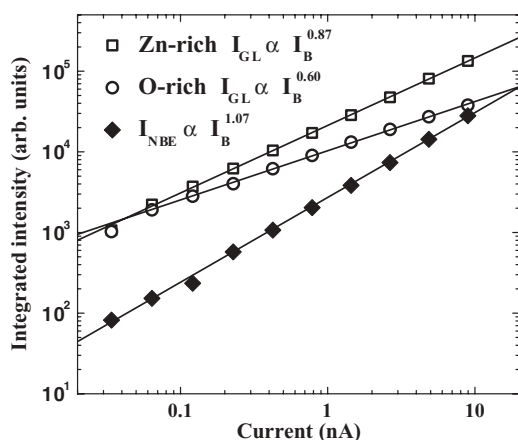


FIG. 3. Log-log plot of GL intensities in Zn- and O-rich ZnO and NBE intensity at 80 K as a function of I_B with a primary electron beam $E_B = 15$ keV, SEM magnification $1000\times$. Power-law fits by straight lines show different I_B dependencies: $I_{GL} \propto I_B^{0.87}$ Zn-rich ZnO, $I_{GL} \propto I_B^{0.60}$ O-rich ZnO and $I_{NBE} \propto I_B^{1.07}$ for both types of ZnO. O-rich GL saturates quickly with increasing I_B , whereas the Zn-rich ZnO has an almost linear dependence, similar to the behavior of the NBE emission.

exhibits a linear dependence on I_B within experimental error for CL measurements, with $k = 1.07 \pm 0.07$, consistent with recombination involving free and bound excitons.³⁰ The strongly sublinear dependence of the O-rich GL is consistent with PL data reported by Guo *et al.*,³¹ who showed that a linear dependence only remained at very low excitation levels. The dynamic behavior of luminescence is thought to be related to the population of recombination centers,^{32,33} the O-rich GL that scales roughly as the square root of excitation density indicates that the V_{Zn} concentration is significantly lower than the V_O concentration. It is worth noting that the positions of both Zn- and O-rich GL peaks remains unchanged with increasing excitation power. The absence of a peak shift indicates that the GL emissions are not a donor-acceptor pair (DAP) recombination but rather a free-to-bound transition.

In the following section, we calculate the recombination rates of the GL recombination channels in Zn- and O-rich ZnO according to the three-energy level model for competitive recombination processes.^{34,35} The inset in Fig. 4 shows three possible recombination channels: one band-to-band and two band-to-deep-state transitions. The NBE emission originates from excitonic recombination (n and p being the concentrations of electrons and holes, respectively). N_T is denoted as the total concentration of deep states, and n_T as the concentration of deep states that are occupied ($n_T \leq N_T$). In the steady state, the balanced equation for the electron concentrations in the conduction band and deep-level state can be expressed as

$$G = V \left(\frac{np}{\tau_a} + \frac{n(N_T - n_T)}{\tau_b} \right), \quad (1)$$

$$\frac{n(N_T - n_T)}{\tau_b} = \frac{n_T p}{\tau_c}. \quad (2)$$

Here, G is electron-hole (e-h) pair generation rate (per cm^3 per second) and $V = b \cdot \tau$, where b is the bimolecular recombination coefficient, and τ characterizes recombination time.³⁵ From time-resolved PL measurements, $b = 10^{-10} \text{ cm}^3 \text{ s}^{-1}$ has

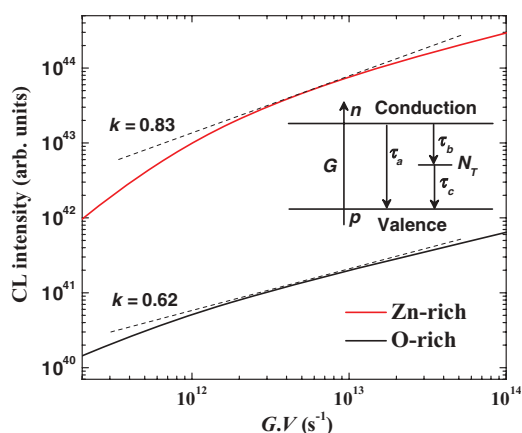


FIG. 4. (Color online) Calculated CL intensities of the GL as a function of the e-h pair generation in the interaction volume at 15 keV. Inset represents the model of three energy levels with their populations n , N_T , and p . τ_a , τ_b , and τ_c are characteristic time constants for three recombination channels. The CL intensities were computed using $\tau_a = 1$ ns, $\tau_b = \tau_c = 5$ ns and $N_T = 10^{18} \text{ cm}^{-3}$ (Zn-rich ZnO) and 10^{15} cm^{-3} (O-rich ZnO). The dashed lines that are tangent to the midregions of the theoretical curves have a slope of 0.83 and 0.62.

been determined for ZnO excitonic recombination.³⁶ Under the excitation conditions described in Sec. III A., the cores of the highly crystalline particles dictate the CL emission, thus the coefficient value for bulk ZnO was used instead of those for ZnO nanostructures.³⁷ Assuming a shallow donor concentration of N_D present in ZnO, the neutrality condition must be satisfied

$$n + n_T = p + N_D. \quad (3)$$

An algebraic manipulation of Eqs. (2) and (3) yields expressions for $n(n_T)$ and $p(n_T)$:

$$n(n_T) = \frac{(N_D - n_T)n_T\tau_b}{n_T\tau_b - (N_T - n_T)\tau_c}, \quad (4)$$

$$p(n_T) = \frac{(N_D - n_T)(N_T - n_T)\tau_c}{n_T\tau_b - (N_T - n_T)\tau_c}. \quad (5)$$

For a given concentration of deep states, n_T can be systematically varied, yielding the corresponding values of n and p . The generation rate G can then be computed from Eq. (1). The bimolecular recombination rates for band-to-acceptor or band-to-donor transitions responsible for the GL are

$$I_{\text{GL}}(\text{acceptor}) \propto \frac{n(N_T - n_T)}{\tau_b}, \quad (6)$$

$$I_{\text{GL}}(\text{donor}) \propto \frac{n_T p}{\tau_c}. \quad (7)$$

Taking into consideration that the radiative lifetime of excitons in ZnO is about 1 ns at 80 K,^{36,38} while the characteristic recombination time of GL varies in the range from 0.2 to 10 ns,^{11,31,37} we used $\tau_a = 1$ ns and $\tau_b = \tau_c = 5$ ns to keep the problem tractable. In CL measurements, it is more useful to work with the e-h pair generation rate in the electron interaction volume, which, to a first approximation, equals the product of the (average) generation rate G and electron interaction volume. In this study the interaction volume was estimated using the Monte Carlo stimulation CASINO.¹⁴ Figure 4 shows the calculated GL intensities as a function of generation rate in the electron interaction volume. The GL intensities exhibit power-law dependences on the e-h pair generation rate. The e-h generation rate in the interaction volume during CL measurements is given by³⁹

$$G.V = \frac{E_B I_B}{E_{e-h} e} (1 - \eta), \quad (8)$$

where E_{e-h} is the mean energy required to create an e-h pair, η is the electron backscattering coefficient, and e is the electronic charge. In general, $E_{e-h} \approx 3E_g$ for semiconductors, where E_g is the band-gap energy.⁴⁰ The product $G.V$ calculated using Eq. (8) and $\eta \approx 0.3$ are on the orders of 10^{11} – 10^{14} s⁻¹ for the CL acquisition conditions used in this study. The extremely high (10^{18} cm⁻³) and low (10^{15} cm⁻³) defect concentrations result in exponent values $k = 0.83$ and 0.62 , respectively, in the midregion of the excitation range. These exponent values are comparable with observed k values for Zn- and O-rich ZnO within experimental error. Note that since the quantum

efficiencies of the GL emissions are not known, the calculated intensities can be shifted vertically without affecting the exponent. Our calculation results indicate that the 2.52-eV defect concentration in Zn-rich ZnO is at least three orders of magnitude greater than the 2.30-eV defect concentration in O-rich ZnO, suggesting V_O is readily formed in a high concentration in the Zn-rich condition. The results are in good agreement with the density functional theory calculations by Zunger *et al.*,^{41,42} which reveal that V_O has the lowest formation energy in Zn-rich ZnO. They are, however, not consistent with the notion that the V_O formation energy is relatively high even under Zn-rich conditions.⁸ It is worth noting that during oxygen annealing, no oxygen evaporation is expected since the O_2 pressure is far greater than the vapor pressure of oxygen in ZnO. Hence, the V_O concentration does not increase, or even decrease (due to potential incorporation of oxygen). Using the bimolecular equation for band-to-band recombination, the exponent was found to vary between 1.00 and 1.16 as this transition remains the primary recombination channel over the e-h generation rate range for both donor and acceptor cases, in good agreement with the measured values for NBE emission. The power-density dependencies of the NBE and GL emissions reveal that small variations in excitation conditions can lead to significant changes to their peak intensity ratio, which varies by an order of magnitude over the excitation power range used in this study. If this ratio is used as a measure of defect concentration, care must be taken that comparisons are carried out under identical excitation conditions. As many optoelectronic applications operate in a high electron injection regime (typically a few hundred amperes per square centimeter), GL emission can become insignificant, especially in the case of V_{Zn} -related GL.

IV. CONCLUSION

In summary, our CL studies show that ZnO exhibits two distinct GL emissions under different stoichiometries. The behaviors of the GL emissions at 2.52 eV in Zn-rich ZnO and at 2.30 eV O-rich ZnO are consistent with band-to-donor and band-to-acceptor transitions, respectively. Combined CL and doping studies reveal the V_{Zn} defect nature of green emission in O-rich ZnO and add weight to the assignment of the Zn-rich GL to V_O . A theoretical model based on competitive recombination processes is developed to arrive at the excitation-power dependencies of the GL emissions. The deep-donor concentration in Zn-rich ZnO is estimated to be three orders of magnitude greater than the deep-acceptor concentration in O-rich ZnO.

ACKNOWLEDGMENTS

Financial support from the Australian Research Council (Grant No. DP0986951) is gratefully acknowledged. The authors thank G. McCredie for technical assistance with hydrogen plasma processing and annealing.

*Corresponding author: cuong.ton-that@uts.edu.au

¹M. H. Huang, S. Mao, H. Feick, H. Q. Yan, Y. Y. Wu, H. Kind, E. Weber, R. Russo, and P. D. Yang, *Science* **292**, 1897 (2001).

²K. Maeda, M. Sato, I. Niikura, and T. Fukuda, *Semicond. Sci. Technol.* **20**, S49 (2005).

³M. Foley, C. Ton-That, and M. R. Phillips, *Appl. Phys. Lett.* **93**, 243104 (2008).

- ⁴K. Vanheusden, C. H. Seager, W. L. Warren, D. R. Tallant, and J. A. Voigt, *Appl. Phys. Lett.* **68**, 403 (1996).
- ⁵A. F. Kohan, G. Ceder, and D. Morgan, *Phys. Rev. B* **61**, 15019 (2000).
- ⁶M. Liu, A. H. Kitai, and P. Mascher, *J. Lumin.* **54**, 35 (1992).
- ⁷D. C. Reynolds, D. C. Look, B. Jogai, and H. Morkoc, *Solid State Commun.* **101**, 643 (1997).
- ⁸A. Janotti and C. G. Van de Walle, *Phys. Rev. B* **76**, 165202 (2007).
- ⁹Y. F. Dong, F. Tuomisto, B. G. Svensson, A. Y. Kuznetsov, and L. J. Brillson, *Phys. Rev. B* **81**, 081201 (2010).
- ¹⁰T. M. Borseth, B. G. Svensson, A. Y. Kuznetsov, P. Klason, Q. X. Zhao, and M. Willander, *Appl. Phys. Lett.* **89**, 262112 (2006).
- ¹¹A. B. Djuricic, Y. H. Leung, K. H. Tam, Y. F. Hsu, L. Ding, W. K. Ge, Y. C. Zhong, K. S. Wong, W. K. Chan, H. L. Tam, K. W. Cheah, W. M. Kwok, and D. L. Phillips, *Nanotechnology* **18**, 095702 (2007).
- ¹²D. Li, Y. H. Leung, A. B. Djuricic, Z. T. Liu, M. H. Xie, S. L. Shi, S. J. Xu, and W. K. Chan, *Appl. Phys. Lett.* **85**, 1601 (2004).
- ¹³C. Ton-That, M. R. Phillips, M. Foley, S. J. Moody, and A. P. J. Stampfl, *Appl. Phys. Lett.* **92**, 261916 (2008).
- ¹⁴D. Drouin, A. R. Couture, D. Joly, X. Tastet, V. Aimez, and R. Gauvin, *Scanning* **29**, 92 (2007).
- ¹⁵J. H. Lim, C. K. Kang, K. K. Kim, I. K. Park, D. K. Hwang, and S. J. Park, *Adv. Mater.* **18**, 2720 (2006).
- ¹⁶H. Zhou, H. Alves, D. M. Hofmann, W. Kriegseis, B. K. Meyer, G. Kaczmarczyk, and A. Hoffmann, *Appl. Phys. Lett.* **80**, 210 (2002).
- ¹⁷B. K. Meyer, H. Alves, D. M. Hofmann, W. Kriegseis, D. Forster, F. Bertram, J. Christen, A. Hoffmann, M. Strassburg, M. Dworzak, U. Haboek, and A. V. Rodina, *Phys. Status Solidi B* **241**, 231 (2004).
- ¹⁸N. Y. Garces, L. Wang, L. Bai, N. C. Giles, L. E. Halliburton, and G. Cantwell, *Appl. Phys. Lett.* **81**, 622 (2002).
- ¹⁹F. Leiter, H. Alves, D. Pfisterer, N. G. Romanov, D. M. Hofmann, and B. K. Meyer, *Physica B* **340**, 201 (2003).
- ²⁰M. G. Wardle, J. P. Goss, and P. R. Briddon, *Phys. Rev. Lett.* **96**, 205504 (2006).
- ²¹C. G. Van de Walle and J. Neugebauer, *Nature (London)* **423**, 626 (2003).
- ²²D. M. Hofmann, A. Hofstaetter, F. Leiter, H. J. Zhou, F. Henecker, B. K. Meyer, S. B. Orlinskii, J. Schmidt, and P. G. Baranov, *Phys. Rev. Lett.* **88**, 045504 (2002).
- ²³E. V. Lavrov, F. Herklotz, and J. Weber, *Phys. Rev. B* **79**, 165210 (2009).
- ²⁴A. Janotti and C. G. Van de Walle, *Nat. Mater.* **6**, 44 (2007).
- ²⁵L. C. L. Lem, C. Ton-That, and M. R. Phillips, *J. Mater. Res.* **26**, 2912 (2011).
- ²⁶X. Liu, X. H. Wu, H. Cao, and R. P. H. Chang, *J. Appl. Phys.* **95**, 3141 (2004).
- ²⁷F. A. Selim, M. H. Weber, D. Solodovnikov, and K. G. Lynn, *Phys. Rev. Lett.* **99**, 085502 (2007).
- ²⁸E. V. Lavrov, J. Weber, F. Bornert, C. G. Van de Walle, and R. Helbig, *Phys. Rev. B* **66**, 165205 (2002).
- ²⁹U. Ozgur, A. Teke, C. Liu, S. J. Cho, H. Morkoc, and H. O. Everitt, *Appl. Phys. Lett.* **84**, 3223 (2004).
- ³⁰M. R. Phillips, *Microchim. Acta* **155**, 51 (2006).
- ³¹B. Guo, Z. R. Qiu, and K. S. Wong, *Appl. Phys. Lett.* **82**, 2290 (2003).
- ³²B. G. Yacobi and D. B. Holt, *Cathodoluminescence Microscopy of Inorganic Solids* (Plenum Press, New York, 1990).
- ³³M. A. Reshchikov and R. Y. Korotkov, *Phys. Rev. B* **64**, 115205 (2001).
- ³⁴M. Omari, A. Gupta, and N. Kouklin, *J. Appl. Phys.* **108**, 024315 (2010).
- ³⁵W. Grieshaber, E. F. Schubert, I. D. Goepfert, R. F. Karlicek, M. J. Schurman, and C. Tran, *J. Appl. Phys.* **80**, 4615 (1996).
- ³⁶T. Serevicius, S. Miasojedovas, V. Gavryushin, and S. Jursenas, *Phys. Status Solidi C* **6**, 2671 (2009).
- ³⁷S. Lettieri, L. S. Amato, P. Maddalena, E. Comini, C. Baratto, and S. Todros, *Nanotechnology* **20**, 175706 (2009).
- ³⁸A. Teke, U. Ozgur, S. Dogan, X. Gu, H. Morkoc, B. Nemeth, J. Nause, and H. O. Everitt, *Phys. Rev. B* **70**, 195207 (2004).
- ³⁹S. M. Davidson, *J. Microsc. (Oxford)* **110**, 177 (1977).
- ⁴⁰R. C. Alig, S. Bloom, and C. W. Struck, *Phys. Rev. B* **22**, 5565 (1980).
- ⁴¹S. B. Zhang, S. H. Wei, and A. Zunger, *Phys. Rev. B* **63**, 075205 (2001).
- ⁴²S. Lany and A. Zunger, *Phys. Rev. B* **78**, 235104 (2008).